



Published in final edited form as:

Neural Netw. 2008 May ; 21(4): 621–627.

Adaptation in Human Balance Control: Lessons for Biomimetic Robotic Bipedes

Arash Mahboobin¹, Patrick J. Loughlin^{1,2}, Mark S. Redfern², Stuart O. Anderson³, Christopher G. Atkeson³, and Jessica K. Hodgins³

¹ Department of Electrical and Computer Engineering, University of Pittsburgh

² Department of Bioengineering, University of Pittsburgh

³ Robotics Institute, Carnegie Mellon University

Abstract

This paper describes mechanisms used by humans to stand on moving platforms, such as a bus or ship, and to combine body orientation and motion information from multiple sensors including vision, vestibular, and proprioception. A simple mechanism, sensory re-weighting, has been proposed to explain how human subjects learn to reduce the effects of inconsistent sensors on balance. Our goal is to replicate this robust balance behavior in bipedal robots. We review results exploring sensory re-weighting in humans and describe implementations of sensory re-weighting in simulation and on a robot.

Keywords

Balance control; posture; sensory re-weighting

1. Introduction

Humans utilize a variety of sensory systems to maintain balance, primary among them being the visual, vestibular and proprioceptive systems. Several studies have demonstrated that human standing posture is affected by perturbations to these sensory systems [1,6,8,11,16, 28], suggesting that feedback control, based on perceived body motion, contributes to postural stability. There is redundancy across these sensory systems and the organization of these feedback control mechanisms is not fully known. Also, there is some question as to whether feedback alone is sufficient for human postural control [2,23], although recent studies have shown that a postural control strategy based solely on sensory feedback can account for experimental findings involving a variety of proprioceptive and visual perturbations to postural control [30,32].

A key finding of human postural control experiments has been that the integration of sensory information appears to be dynamically regulated to adapt to changing environmental conditions

Mailing Address For Proofs And Reprints: Chris Atkeson, CMU RI, 5000 Forbes Avenue, Pittsburgh, PA, 15213, USA, Email preferred: cga@cmu.edu, Tel.: ¹(412) 624-8000; ²(412) 624-4771, ³(412) 268-3818, Fax: ¹(412) 624-8003; ²(412) 647-0108, ³(412) 268-6436, Email: arm19@pitt.edu, loughlin@enr.pitt.edu, mredfern@pitt.edu soa@cs.cmu.edu, cga@cmu.edu, jkh@cs.cmu.edu.

Publisher's Disclaimer: This is a PDF file of an unedited manuscript that has been accepted for publication. As a service to our customers we are providing this early version of the manuscript. The manuscript will undergo copyediting, typesetting, and review of the resulting proof before it is published in its final citable form. Please note that during the production process errors may be discovered which could affect the content, and all legal disclaimers that apply to the journal pertain.

and available sensory information, a process sometimes referred to as “sensory re-weighting” [6,30,32,34,19,12,27,20]. For example, during eyes-closed stance on a fixed, level surface, the primary sensory source for information about body orientation in space is proprioceptive, but under conditions where the platform moves, the primary source of sensory information shifts from proprioceptive to graviceptive/vestibular [30].

Current humanoid robots move more slowly than humans and are much less stable [25,24,18,4,9,26]. The control algorithms are typically not designed to handle large perturbations or ambiguous sensory information, two components often seen in human balance experiments and daily activity. Instead, the floor is assumed to be level, stiff, and not in motion. Independent and decoupled simple linear controllers for each joint (joint-level PD control) with only proprioceptive feedback form the core of robot standing balance control, and the size of the perturbations are limited so that decoupled linear control is adequate. Some robots use force control to implement a more compliant ankle [4,10,17] which is useful for stepping on uneven terrain, but not for standing vertically. There is often only one response strategy to choose from, typically using ankle torques to adjust the center of pressure (the ankle strategy). One exception to this are the Honda robots, which can take a step in response to a large perturbation [4]. More advanced schemes have been proposed but not yet implemented [5,7,13].

We note a major difference between current robots and humans in how balance is maintained. In robotics, the emphasis has been on controlling the location of the center of pressure based on proprioception, with little use of vestibular signals and no use of vision. In humans, vestibular and visual signals are also important [30]. The multiple sensory sources allow for more complex sensorimotor strategies not seen in humanoid robots, and arguably contribute to robust human balance function across a variety of environments and perturbations.

2. Human Postural Control And Sensory Re-weighting

Human postural control has been studied for over fifty years, with conceptual and computational models being developed. These models have led to advances in the diagnosis and management of balance disorders. A variety of models have been proposed and continue to be developed (e.g., [8,30,34,14,15,33,29,31,21,22]). Many models are developed in accordance with specific experimental conditions; while no single model explains all aspects of human postural control, the model [30] we consider in detail here has been shown to accurately fit experimental data in a variety of conditions, both steady-state [30] and transient [32]. Moreover, the model provides a conceptually simple, yet experimentally supported, concept of sensory adaptation/re-weighting.

The model (Fig. 1) consists of a linearized (i.e., small angle) single-link inverted pendulum representation of body dynamics. Upright stance is maintained by a corrective torque applied about the ankle joint, generated by a proportional-integral-derivative (PID) controller, with fixed gain parameters K_P , K_I and K_D . Note that the model utilizes both position and velocity information to stabilize the inverted pendulum, consistent with control theory.

The parameters K_P and K_D represent the active stiffness and damping, respectively, of the postural control system. They are termed “active” because they generate corrective torque in response to an external perturbation, in contrast to passive stiffness and damping of the muscles and tendons during quiet standing. The contributions of the passive stiffness and damping to torque generation have been found to be negligible during perturbations (a factor of ten smaller than the active torque generation) and can be dropped from the model [30,31]. The parameter t_d in the model represents the effective time delay of the system, which includes combined delays due to sensory transduction, neural transmission, nervous system processing, muscle activation, and force development.

If all of the sensory systems are modeled as having no dynamics over the bandwidth of body sway movement (i.e., taken as unity), then the sensory error signal E is

$$E(t) = W_v(VS(t) - BS(t)) + W_p(SS(t) - BS(t)) - W_g(BS(t)) \quad (1)$$

where BS , VS and SS are angles, with respect to earth-vertical, of the body, visual scene and support surface, respectively, as shown in the stick-figures in Fig. 1, and W_v , W_g and W_p are the sensory weights for the visual, graviceptive (vestibular), and proprioceptive sensory systems, respectively.

For healthy subjects with intact sensory organs and perturbations limited in magnitude and bandwidth to those often used in experimental studies of human postural control (e.g., [30, 32]), this “no dynamics” assumption for the sensory systems is reasonable. This assumption simplifies the sensory integration strategy, which is modeled via the sensory weights W_v , W_g and W_p . Unlike the fixed PID gains of the controller, the sensory weights can change with environmental conditions (the “sensory re-weighting” strategy). These sensory weights represent the *relative* contribution of each sensory channel to postural control.

For the model, the body sway (BS) in response to support surface (SS) or visual scene (VS) motion is given in the Laplace domain by

$$BS(s) = H(s) [W_p SS(s) + W_v VS(s)] \quad (2a)$$

where s is the Laplace variable and

$$H(s) = \frac{(K_D s^2 + K_P s + K_I) e^{-s\tau_d}}{Js^3 - mghs + W(K_D s^2 + K_P s + K_I) e^{-s\tau_d}} \quad (2b)$$

is the unity-gain transfer function of the postural control feedback model.

A key concept of the model and the sensory re-weighting hypothesis is the *effective overall sensory weight*, \mathbf{W} , of the system, which is the sum of the sensory weights of *those channels that contribute accurate sensory information about body sway* (BS). For example, the effective overall sensory weight is $\mathbf{W} = W_p + W_g + W_v$ during eyes-open quiet standing on a fixed platform. But, for eyes-closed stance, the visual system does not contribute information about body sway, so the effective overall sensory weight in this case is $\mathbf{W} = W_p + W_g$. For stance on a sway-referenced platform, on which the support surface rotates in one-to-one proportion to body sway ($SS = BS$ in Fig. 1), the proprioceptive channel does not contribute accurate information about body sway, so in this case the effective overall sensory weight is $\mathbf{W} = W_g + W_v$. Thus, the sensory weights that contribute to the effective overall sensory weight are different under different environmental conditions (i.e., under different manipulations of the sensory inputs). An important point to appreciate is that as the value of \mathbf{W} changes, the dynamics of body sway will change. In particular, during transient conditions the system can be pushed towards instability if sensory re-weighting is inadequate, causing \mathbf{W} to be too large or too small, as discussed further below.

2.1. Steady-state vs. transient conditions

The sensory re-weighting hypothesis holds that, under *steady-state* conditions, the effective overall sensory weight is unity, $\mathbf{W} = 1$ (this is a torque normalization constraint that results in non-oscillatory dynamics of body sway) [30]. For example, for stance with eyes closed on a fixed platform, $\mathbf{W} = W_p + W_g = 1$ during steady-state. However, during *transient* conditions, in particular following a sudden change in the available sensory information, \mathbf{W} will differ from unity for a period of time until the sensory integration process adjusts the weights of the

sensory systems to compensate for the transient change in sensory information [32]. For example, for the eyes-closed stance condition, if the platform suddenly transitions from fixed to sway-referenced, then the effective overall sensory weight becomes $\mathbf{W} = W_g$, and this is initially less than unity. If \mathbf{W} is not unity, then either too much or too little corrective torque will be generated and oscillatory sway will occur at specific frequencies. This oscillatory sway persists until the sensory integration process re-establishes $\mathbf{W} = 1$. The tendency of a system to oscillate at a particular frequency is called “resonance” and is reflected by a peak in the system’s frequency response at that frequency; the sharper the peak, the more “resonant” the system and the stronger and more sustained are the oscillations. Increased resonance is characteristic of a system nearing instability. This effect of changes in the value of \mathbf{W} on the body sway that develops is illustrated in the frequency response magnitude plots shown in Fig. 2. Note that the model predicts oscillatory body sway at specific frequencies if sensory re-weighting is inappropriate (\mathbf{W} less than or greater than one).

3. Experimental Results: Sensory Re-weighting In Healthy Young Adults

Under experimental conditions where the sensory input to the postural control system was deliberately altered, transient periods of low or high frequency oscillations in the body sway of healthy young adults were observed [32]. Shown in Fig. 3 (left) are body sway measurements and the corresponding time-varying spectrum (or time-frequency distribution) obtained during eyes-closed stance on a platform that transitioned from fixed, to sway referenced for 60 seconds (labeled SR SS in Fig. 3), and then back to fixed. (See [32] for details of the experimental protocol, methodology and data analysis.)

The oscillations observed experimentally were interpreted by Peterka and Loughlin [32] in terms of the model discussed above and in their paper as follows. During the initial period of eyes-closed stance on the fixed platform, the effective overall sensory weight is $\mathbf{W} = W_p + W_g$, and under the sensory re-weighting hypothesis, once steady-state has been reached we have $W_p + W_g = 1$. Following the transition to the sway-referenced platform (starting at 60 seconds in the figure), the proprioceptive channel no longer provides accurate information about body sway. Hence the effective overall sensory weight becomes $\mathbf{W} = W_g$ which will be less than unity immediately after the transition to sway-referencing. The frequency response of the model (Fig. 2, dashed line) shows that a decrease in the value of \mathbf{W} will cause a change in the frequency characteristics of sway, manifest by a low frequency resonance. This resonant behavior of the model for low values of \mathbf{W} is consistent with the experimentally observed body sway oscillations in the time-varying spectrum of Fig. 3 (left; note the band of energy in the TFD plot around 0.1 Hz that develops after $t=60$ s). As the body adjusts to the sway-referenced condition over time, sensory re-weighting brings the effective sensory weight back to unity, i.e., the graviceptive weight W_g increases to near unity. Upon the transition back to a fixed platform (at $t = 120$ sec), the effective sensory weight becomes $\mathbf{W} = W_p + W_g$, but now the graviceptive weight is higher than it was during the initial fixed platform condition ($t < 60$ s), so that now $\mathbf{W} > 1$. In the model, this results in oscillatory sway near 1 Hz (Fig. 2, dot-dashed curve), similar to what was observed experimentally (see the time-varying spectrum in Fig. 3 (left) and in particular the band of energy that develops around 1 Hz after $t=120$ s). A simulation from the model of these experimental conditions and postulated sensory re-weighting is shown in Fig. 3 (right). The good match between model predictions and experimental results inspires some confidence that the model captures important attributes of sensorimotor integration in postural control.

As discussed by Peterka and Loughlin [32], another interpretation of these results is suggested by the model. Rather than re-weighting sensory information, it is possible that the postural control system scales the controller gains to generate the torque necessary to compensate for transitions to different environments. According to this “load compensation” strategy, as it is

called, the amount of corrective torque changes as necessary, but the relative contributions of the different sensory systems remain fixed, independent of environmental conditions. Interestingly, under ideal experimental conditions (i.e., when sway-referencing is perfect, which is not possible in practice), either strategy in the model – load compensation or sensory re-weighting – can generate low or high frequency oscillations, such that it is not possible to differentiate between the two strategies. However, if the model incorporates realistic conditions of sway-referencing (by modeling platform actuator dynamics with a second-order transfer function fit to measured input-output platform responses), the two strategies in the model generate different resonances during sway-referencing, and it is possible to distinguish between the two strategies. The model results generated by the load compensation strategy were not consistent with the experimental results, thereby lending further support to the sensory re-weighting interpretation [32].

4. Robot Control Utilizing Manual Sensory Re-weighting

We have implemented a preliminary sensory re-weighting control strategy similar to that described in [30,32] on a bipedal robot. This preliminary implementation used the robot sensors directly, rather than attempting to simulate biological signals. To test the model, the robot was placed on a standard clinical balance testing platform (Fig. 4), and controller gains were set to maintain stability, with proprioceptive (ankle angle) and graviceptive (inertial) sensory weights initially set to 0.6 and 0.4, respectively (Fig. 4 right). The proprioceptive and graviceptive gains are consistent with reports in the literature that during quiet standing with eyes closed, proprioception seems to be the dominant source of sensory information for standing balance in humans.

The platform is initially fixed, and at a certain point (10 seconds in Fig. 4) begins sway referencing: rotating in direct 1:1 proportion to body angle about an axis collinear with the ankle joint of the robot. This behavior has the effect of eliminating reliable ankle proprioception, because the ankle angle remains at approximately 90 degrees, independent of body sway. A feedback control strategy that utilizes primarily ankle proprioception would result in the robot falling shortly after the platform transitions to the sway-referenced condition, as indeed occurred when re-weighting was not used (Fig. 4). We note that it is not unusual for human subjects to also lose their balance the first time they experience a sway-referenced platform with eyes closed.

To maintain balance, the source of sensory information must be rapidly switched from ankle proprioception to the graviceptive sensors, which provides a measure of body angle with respect to earth vertical. We manually implemented sensory re-weighting in the robot model, so that at the transition of the platform from fixed to sway-referenced, the graviceptive gain increased and the proprioceptive ankle gain decreased. This strategy resulted in stable stance for the robot on the sway-referenced platform (Fig. 4). This implementation demonstrates that sensory re-weighting is a feasible solution that can be implemented on a physical system with its real world noise and unmodeled dynamics.

5. Sensory Re-weighting In An Optimal Filtering Context

In this section we put sensory re-weighting in an optimal filtering context. The Kalman filter provides a way to combine noisy sensors, given certain assumptions [3]. Given estimates of sensor noise and disturbance size, the filter design process automatically generates sensory weights. The goal of this section is to see whether sensory weights produced in this way work on the robot. Future work will explore automatic approaches to estimating sensor noise levels and disturbance size, and thus automatic generation of sensory weights.

Fig. 5 is a block diagram of a model for standing balance in a humanoid robot. For simplicity, the robot dynamics are modeled as a single link inverted pendulum, where the states (angle and angular velocity) of the inverted pendulum are defined with respect to vertical. To maintain an upright position a controlling torque (u) is applied at the ankle joint. The torque is generated by state feedback $u = -\mathbf{K}\hat{x}$, where \mathbf{K} is the state feedback gain matrix and \hat{x} is the state estimate. The state feedback gain is designed to match the natural frequency ($\omega_n = 2.02$ radians/second) and damping ratio ($\zeta = 1.06$) found in human experiments [30]. The robot's mass multiplied by the height of its center of mass is $m_{cm} = 34.29$ Kg-m, and its moment of inertia about the ankle is $J = 52.39$ Kg-m². The position and velocity gains are given by:

$$K_p = \omega_n^2 J + m_{cm} g \quad (3a)$$

$$K_d = 2\zeta \omega_n J \quad (3b)$$

resulting in $\mathbf{K} = [551 \ 225]$ (g is 9.81m/s^2)

State estimates are obtained from a Kalman filter, where the inputs are the noisy sensory channels as well as the ankle torque (Fig. 5). The Kalman filter dynamics have the same basic structure as the robot dynamics but with an additional input $y - \hat{y}$:

$$\begin{aligned} \hat{\dot{x}} &= A\hat{x} + Bu + L(y - \hat{y}) \\ \hat{y} &= C\hat{x} \end{aligned} \quad (4)$$

where \hat{x} is the state estimate (which includes the estimated angle and angular velocity), u is the ankle torque, A and B are the linearized robot dynamics, C is a matrix indicating how sensor measurements depend on the state, y is the noisy sensory measurements, and \hat{y} is the predicted sensory measurements. The Kalman filter gain L is obtained from

$$L = P_L C^T R_L^{-1} \quad (5)$$

where P_L is a positive definite matrix that is the solution to the Riccati equation

$$0 = AP_L + P_L A^T + Q_L - P_L C^T R_L^{-1} C P_L \quad (6)$$

Q_L and R_L represent the process (w) and sensor (v) noise covariance matrices, respectively. The process noise is obtained from $Q_L = GQ_w G^T$, where Q_w represents the noise variance of w and G indicates how the process noise affects the state. In our work R_L is a square diagonal matrix where each element on the diagonal represents the noise variance of the corresponding sensor channel.

The model includes two sensory channels: the proprioceptive (ankle) and graviceptive (vestibular) channels. We assume that each sensory channel senses both position and velocity of the robot and that the channels have no dynamics over the bandwidth of body sway movement. These assumptions result in a sensor noise covariance matrix R_L :

$$R_L = \begin{bmatrix} v_p & 0 & 0 & 0 \\ 0 & v_p & 0 & 0 \\ 0 & 0 & v_g & 0 \\ 0 & 0 & 0 & v_g \end{bmatrix} \quad (7)$$

where v_p , v_p , v_g , and v_g represent the noise variance of the proprioceptive (p) and graviceptive (g) angle and angular velocity signals.

To simulate spontaneous sway, we have included process noise (w) with variance $Q_w = 0.002$. To perturb the proprioceptive sensory system we have included an external disturbance d which

moves the foot. Because we model the ankle as a pure torque source, this perturbation does not affect the body directly, but only affects the proprioceptive measurement of joint angle and joint angular velocity.

To design the Kalman filter, the covariance on the sensor noise is

$$\mathbf{R}_{L_1} = \begin{bmatrix} 0.14 & 0 & 0 & 0 \\ 0 & 0.14 & 0 & 0 \\ 0 & 0 & 65 & 0 \\ 0 & 0 & 0 & 0.21 \end{bmatrix} \quad (8)$$

where the noise covariance for the graviceptive channel is as reported in [34]. This design leads to Kalman filter gains of

$$\mathbf{L}_1 = \begin{bmatrix} 0.0043 & 0.0110 & 0.0000 & 0.0073 \\ 0.0110 & 0.0278 & 0.0000 & 0.0185 \end{bmatrix} \quad (9)$$

We choose the ratio of the velocity elements of \mathbf{R} to get a ratio of 60/40 in the proprioceptive vs. graviceptive elements of \mathbf{L}_1 , which roughly matches human sensor weightings [30]. We have found that scaling \mathbf{R} as a whole has little effect on the Kalman filter gains, probably due to the fact that the controlled system is unstable. To handle proprioceptive perturbations, we design a second Kalman filter with sensor noise covariance and gains:

$$\mathbf{R}_{L_2} = \begin{bmatrix} 0.49 & 0 & 0 & 0 \\ 0 & 0.49 & 0 & 0 \\ 0 & 0 & 65 & 0 \\ 0 & 0 & 0 & 0.21 \end{bmatrix} \quad (10)$$

$$\mathbf{L}_2 = \begin{bmatrix} 0.0023 & 0.0057 & 0.0000 & 0.0134 \\ 0.0057 & 0.0145 & 0.0000 & 0.0339 \end{bmatrix} \quad (11)$$

In this case the estimate of the strength of proprioceptive sensor noise was increased, so that the ratio of proprioceptive to graviceptive velocity elements in \mathbf{L} is roughly 30/70, matching human sensor weightings during ankle perturbations.

We now present a simulation for the model described above. The external disturbance (platform perturbation) applied to the ankle has a total duration of 181 seconds and consists of two cycles of a pseudorandom ternary sequence (PRTS: random sequence of 0, $-n$, $+n$) preceded and followed by 30 seconds of no disturbance (Fig. 6). Each cycle of the PRTS is 60.5 seconds with a 2-degree peak-to-peak amplitude. The body sway angle resulting from the external disturbance to the model is plotted in Fig. 7, where the vertical black dashed line indicates onset of sensory re-weighting (switching Kalman filter gains from \mathbf{L}_1 to \mathbf{L}_2). As evident from the graph, after about 70 seconds into the perturbation, where sensory re-weighting has occurred, the model is able to lower the amount of body sway and rely more on the less noisy channels available.

Fig. 8 shows this experiment applied to the robot. The gains had to be changed slightly from the simulation to compensate for additional damping in the actuation and other unmodeled dynamics $\mathbf{K} = [700 \ 150]$. We see that Fig. 7 and 8 show similar performance improvements due to sensory re-weighting. This implementation demonstrates that an optimal filtering approach to sensory re-weighting is also a feasible solution that can be implemented on a physical system with its real world noise and unmodeled dynamics.

6. Discussion

We have described our work in modeling human balance control by applying sensory re-weighting to robots. Our long term goal is to develop computational theories of how the weights in sensory re-weighting are chosen. Models of this process are conspicuously absent from work on human balance control, and are necessary for robot balance control.

One lesson from human balance control is that sensory re-weighting is a simple mechanism to handle a wide variety of perturbations: standing on a moving bus, watching a moving scene, or handling the effects of self motion on inertial sensing. Different sensory channels are more or less sensitive to different types of perturbations, and thus different types of perturbations can be compensated for by weighting the various sensory channels. An accurate model of the disturbance, sensors, or dynamics of the system is not needed. For example, it is not necessary to accurately estimate the platform angle in order to stand during ankle perturbations.

Sensory re-weighting provides a way to combine many sensory systems. Humans use proprioception, inertial sensing, and vision to stand robustly. Robots typically rely on only one or two sensory systems. Another function of sensory re-weighting is to handle inconsistent or malfunctioning sensors.

An important step towards robust robot behavior is developing mechanisms to handle erroneous, inconsistent, or malfunctioning sensors. An important question to be addressed is how sensory re-weighting might be accomplished. We have outlined an approach based on optimal filter design, in which sensor noise and disturbance size estimates are automatically generated and generate corresponding sensory weights. We discuss here another possible strategy that we believe is physiologically plausible. The approach is based on a comparison between sensory channels, in order to determine disagreement between the channels with respect to sensed body sway. To illustrate the concept, consider the difference between the proprioceptive and graviceptive sensory channels in Fig. 1, under eyes-closed stance on a fixed platform. The graviceptive channel senses body sway with respect to earth vertical (BS in the model), while the proprioceptive channel senses body sway with respect to the support surface (SS-BS in the model). Hence, the sensory difference gives us a measure of platform motion, SS, which is zero for the fixed platform condition, and the two sensory channels are in agreement with each other. However, during sway referencing, the vestibular channel continues to sense true body sway but the proprioceptive channel senses no sway (assuming ideal sway-referencing, for which $SS = BS$), such that the sensory difference is no longer zero but rather is equal to BS. This disagreement between the sensors can be detected by comparing the (rectified and possibly filtered difference signal) to some threshold, after which changes in the sensory gains can be initiated. We are currently investigating this approach.

Acknowledgements

This work supported in part by the National Science Foundation under NSF Grants CNS-0224419, DGE-0333420, and ECS-0325383. Also supported in part by funding from the Pittsburgh Claude D. Pepper Older Americans Independence Center [P30 AG024827 (NIA)].

References

1. Day BL, Severac Cauquil A, Bartolomei L, Pastor MA, Lyon IN. Human body-segment tilts induced by galvanic stimulation: A vestibularly driven balance protection mechanism. *Journal of Physiology* 1997;500:661–672. [PubMed: 9161984]
2. Fitzpatrick R, Burke D, Gandevia SC. Loop gain of reflexes controlling human standing measured with the use of postural and vestibular disturbances. *Journal of Neurophysiology* 1996;76:3994–4008. [PubMed: 8985895]

3. Grewal, MS.; Andrews, AP. Kalman filtering: Theory and practice using Matlab. 2. John Wiley & Sons; 2001.
4. Hirai, K.; Hirose, M.; Haikawa, Y.; Takenaka, T. The development of Honda humanoid robot. Proceedings of the IEEE International Conference on Robotics and Automation; 1998. p. 1321-1326.
5. Hofmann, A.; Massaquoi, S.; Popovic, M.; Herr, H. A sliding controller for bipedal balancing using integrated movement of contact and non-contact limbs. IEEE/RSJ International Conference on Intelligent Robots and Systems; 2004. p. 1952-1959.
6. Horak, FB.; Macpherson, JM. Handbook of Physiology: Section 12: Exercise: Regulation and Integration of Multiple Systems. New York: Oxford University Press; 1996. Postural orientation and equilibrium; p. 255-292.
7. Ito, S.; Nishigaki, T.; Kawasaki, H. Upright posture stabilization by ground reaction force control. Proceedings of the International Symposium On Measurement, Analysis and Modeling of Human Functions; 2001. p. 515-520.
8. Johansson R, Magnusson M. Human postural dynamics. IEEE Transactions on Biomedical Engineering 1991;18:413-437.
9. Kaneko, K.; Kanehiro, F.; Kajita, S.; Hirukawa, H.; Kawasaki, T.; Hirata, M.; Akachi, K.; Isozumi, T. Humanoid robot HRP-2. Proceeding of the IEEE International Conference on Robotics and Automation; 2004. p. 1083-1090.
10. Kajita, S.; Yokoi, K.; Saigo, M.; Kazuo, T. Balancing a humanoid robot using backdrive concerned torque control and direct angular momentum feedback. Proceedings of the IEEE International Conference on Robotics and Automation; 2001. p. 3376-3382.
11. Kavounoudias A, Gilhodes JC, Roll R, Roll JP. From balance regulation to body orientation: two goals for muscle proprioceptive information processing? Experimental Brain Research 1999;124:80-88.
12. Kiemel T, Oie KS, Jeka JJ. Multisensory fusion and the stochastic structure of postural sway. Biological Cybernetics 2002;87:262-77. [PubMed: 12386742]
13. Kudoh, S.; Komura, T.; Ikeuchi, K. The dynamic postural adjustment with the quadratic programming method. Proceedings of 2002 IEEE/RSJ International Conference on Intelligent Robots and Systems; 2002. p. 2563-2568.
14. Kuo AD. An optimal control model for analyzing human postural balance. IEEE Transactions on Biomedical Engineering 1995;42:87-101. [PubMed: 7851935]
15. Kuo AD. An optimal state estimation model of sensory integration in human postural balance. Journal of Neural Engineering 2005;2:S235-S249. [PubMed: 16135887]
16. Lee DN, Lishman JR. Visual proprioceptive control of stance. Journal of Human Movement Studies 1975;1:87-95.
17. Lim, H.; Setiawan, S.; Takamishi, A. Biped walking using stabilization and compliance control. Proceedings of the 2001 IEEE-RAS International Conference on Humanoid Robots; 2001.
18. Lofler K, Gienger M, Pfeiffer F. Sensors and control concept of walking Johnnie. International Journal of Robotics Research 2003;22:229-239.
19. Mahboobin, A.; Beck, C.; Moeinzedah, M.; Loughlin, PJ. Analysis and validation of a human postural control model. Proceedings of the American Control Conference; 2002. p. 4122-4128.
20. Mahboobin A, Loughlin PJ, Redfern MS, Sparto PJ. Sensory re-weighting in human postural control during moving-scene perturbations. Experimental Brain Research 2005;167:260-267.
21. Mergner T, Maurer C, Peterka RJ. A multisensory posture control model of human upright stance. Progress in Brain Research 2003;142:189-201. [PubMed: 12693262]
22. Mergner T, Schweigart G, Maurer C, Blümler A. Human postural responses to motion of real and virtual visual environments under different support base conditions. Experimental Brain Research 2005;167:535-556.
23. Morasso PG, Baratto L, Capra R, Spada G. Internal models in the control of posture. Neural Networks 1999;12:1173-1180. [PubMed: 12662652]
24. Nagasaka, K.; Kuroki, Y.; Suzuki, S.; Itoh, Y.; Yamaguchi, J. Integrated motion control for walking, jumping and running on a small bipedal entertainment robot. Proceedings of the 2004 IEEE International Conference on Robotics & Automation; 2004. p. 3189-3194.

25. Nishiwaki, K.; Kagami, S.; Kuffner, JJ.; Inaba, M.; Inoue, H. Humanoid 'jsk-h7': Research platform for autonomous behavior and whole body motion. Proceedings of the Third IARP International Workshop on Humanoid and Human Friendly Robotics; 2002. p. 2-9.
26. Ogura, Y.; Aikawa, H.; Lim, H.; Takanishi, A. Development of a human-like walking robot having two 7-dof legs and a 2-dof waist. Proceedings of the 2004 IEEE International Conference on Robotics & Automation; 2004. p. 134-137.
27. Oie KS, Kiemel T, Jeka JJ. Multisensory fusion: simultaneous re-weighting of vision and touch for the control of human posture. *Cognitive Brain Research* 2002;14:164–76. [PubMed: 12063140]
28. Peterka RJ, Benolken MS. Role of somatosensory and vestibular cues in attenuating visually induced human postural sway. *Experimental Brain Research* 1995;105:101–110.
29. Peterka RJ. Postural control model interpretation of stabilogram diffusion analysis. *Biological Cybernetics* 2000;82:335–343. [PubMed: 10804065]
30. Peterka RJ. Sensorimotor integration in human postural control. *Journal of Neurophysiology* 2002;88:1097–1118. [PubMed: 12205132]
31. Peterka RJ. Simplifying the complexities of maintaining balance. *IEEE Engineering in Medicine and Biology Magazine* 2003;22:63–68. [PubMed: 12733461]
32. Peterka RJ, Loughlin PJ. Dynamic regulation of sensorimotor integration in human postural control. *Journal of Neurophysiology* 2004;91:410–423. [PubMed: 13679407]
33. Van der Kooij H, Jacobs R, Koopman B, Grootenboer H. A multisensory integration model of human stance control. *Biological Cybernetics* 1999;80:299–308. [PubMed: 10365423]
34. Van der Kooij H, Jacobs R, Koopman B, Van der Helm F. An adaptive model of sensory integration in a dynamic environment applied to human stance control. *Biological Cybernetics* 2001;84:103–115. [PubMed: 11205347]

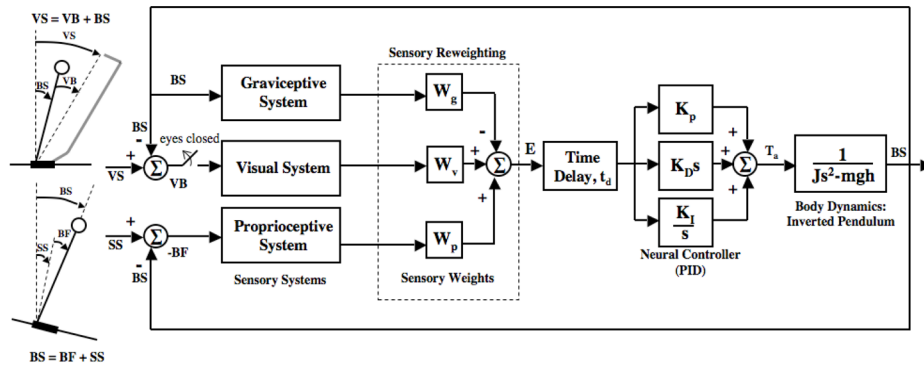


Fig. 1. Feedback model of postural control. The body is modeled as a linearized inverted pendulum. The sensory pathways include variable sensory weights (W_g, W_v, W_p) that can change as environmental factors change (the “sensory re-weighting” hypothesis). BS, VS and SS are angles, with respect to earth-vertical, of the body, visual scene and support surface, respectively, as shown in the stick-figures. VB and BF are the relative angles of the visual scene and the support surface with respect to the body. Corrective torque about the ankle, T_a , is generated by a proportional-integral-derivative (PID) controller with fixed gains K_p, K_D, K_I , acting on the combined delayed sensory error signal E. Modified from [30] and [32].

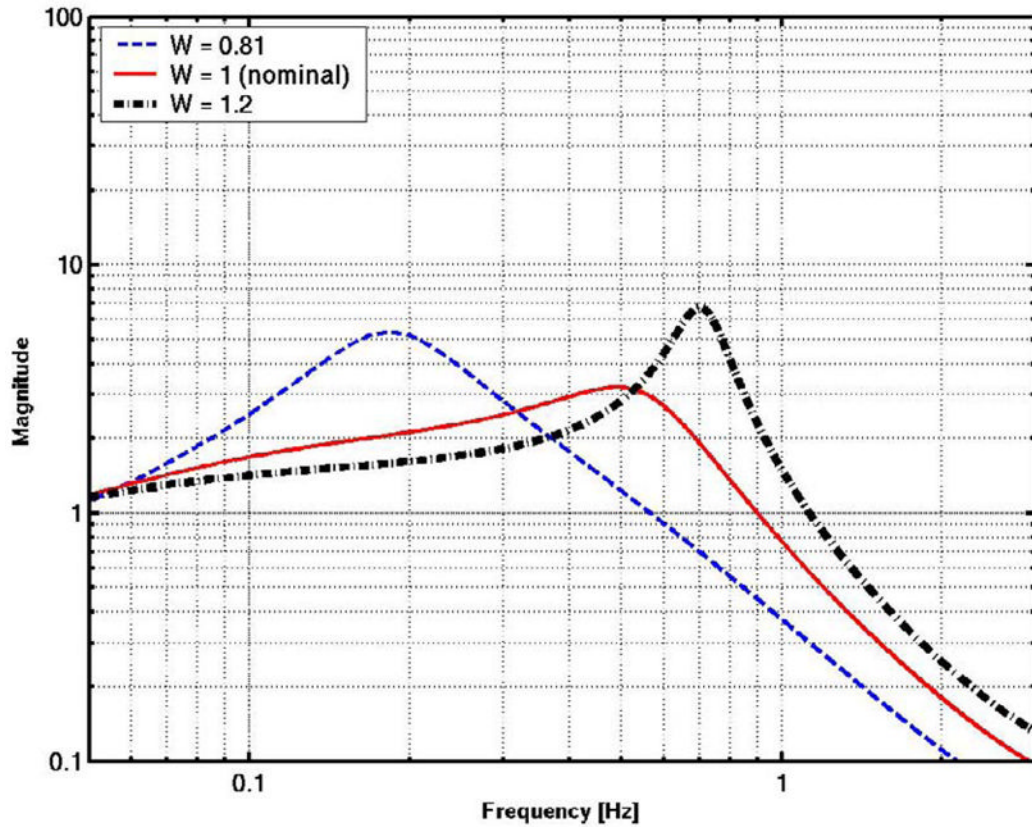


Fig. 2. Frequency response plots for the postural control model in Fig. 1, showing the effects of changes in the effective overall sensory weight, \mathbf{W} . Dotted curve is for $\mathbf{W} = 0.81$, solid is for $\mathbf{W} = 1$, dotted-dashed is for $\mathbf{W} = 1.2$. PID control parameters were the same in all cases [$K_P = 18.1$ N-m/deg, $K_I = 2.2$ N-m/deg-s, $K_D = 6.1$ N-m-s/deg], as were other physical parameters [$g = 9.8$ m/s², $m = 83$ Kg, $h = 0.9$ m, $J = 81$ Kg-m²]. Note the changes in the frequency response as \mathbf{W} changes, and in particular the development of resonances (peaks in the frequency response) at particular frequencies for $\mathbf{W} > 1$ and $\mathbf{W} < 1$.

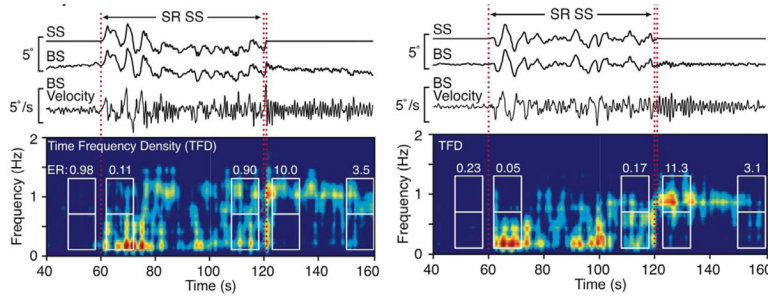


Fig 3. Time series and corresponding time-varying spectra (or time-frequency distributions (TFD), bottom plots) of postural sway from a subject (LEFT) and from the model (RIGHT). The support surface angle (SS) is sway-referenced (SR) during the period 60–120 s. After rapidly returning to a fixed support surface within 1 s (denoted by the double vertical dotted lines at 120 s), body sway oscillations at ~1 Hz develop (orange-yellow band in the TFD around 1 Hz for $t > 120$ s), indicative of inadequate sensory re-weighting. (Boxed areas in the TFD correspond to time-frequency regions of interest for which energy ratios (ER) of high-frequency (0.7–1.3 Hz) to low-frequency (0.1–0.7 Hz) energy were analyzed; numbers above the box reflect the ER values.) Adapted from [32].

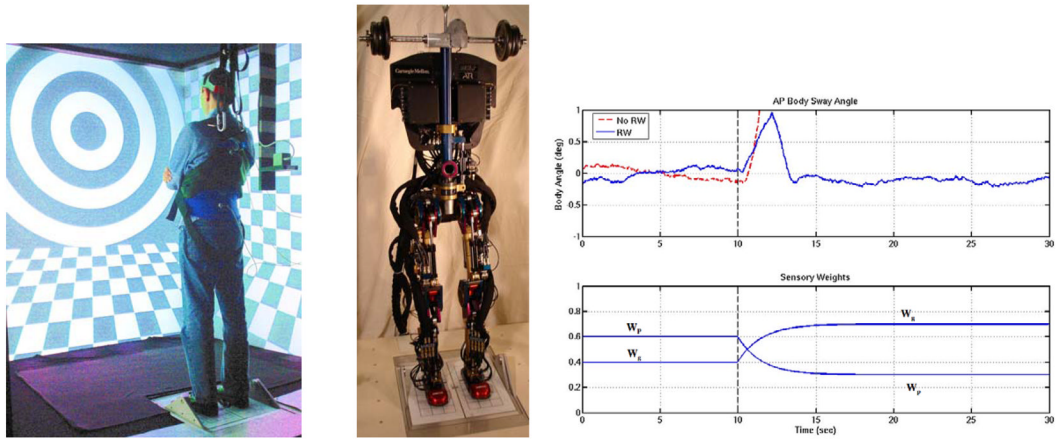


Fig. 4. Left: An experimental subject standing on a clinical balance platform (Equitest) in a visual “cave”. Middle: Our bipedal robot standing on an identical balance platform. Right: Preliminary results on robot balancing during sway referencing, which tilts the support platform to keep the ankle angle at 90° . The top graph plots body angle in two trials, and the vertical dashed line indicates the onset of sway-referencing. The first trial (dashed red line) is with fixed feedback gains, and the robot quickly falls. The second trial (solid blue line) is with sensory re-weighting where the weight on the now misleading ankle sensor is reduced. The bottom graph plots the manually specified sensor weightings for proprioception (W_p) and graviception (W_g) during sensory re-weighting. When sensory re-weighting is not used the weights are held constant at their initial values (0.6, 0.4).

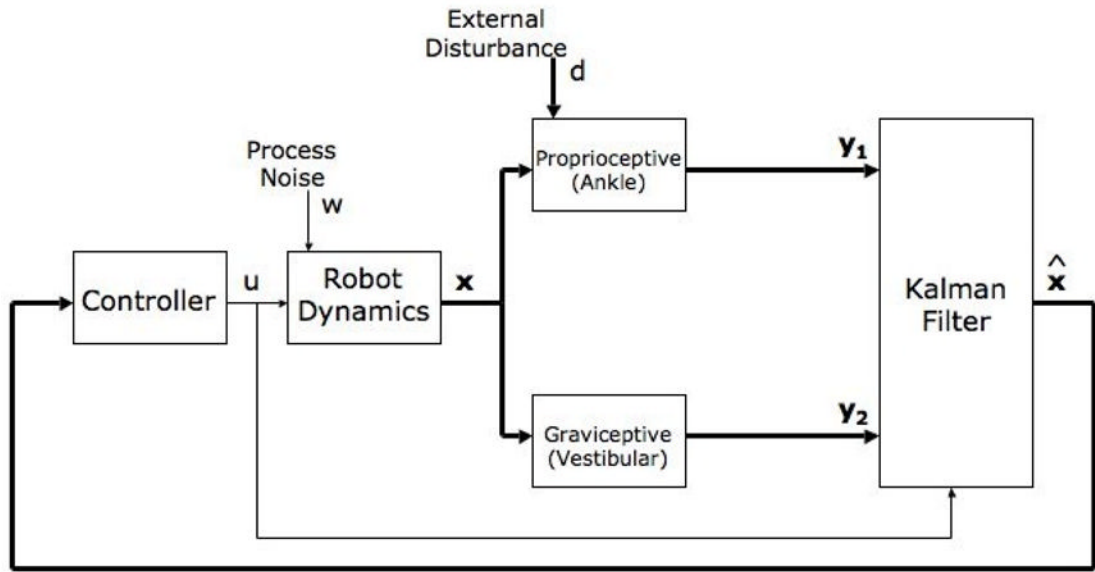


Fig. 5. Block diagram of a model for standing balance, where vector elements are represented by bold letters and lines. The robot dynamics are modeled as a single-link inverted pendulum. The model includes two sensory channels, namely the proprioceptive (ankle) and graviceptive (vestibular), where both channels are assumed to sense position and velocity. The ankle torque u is generated by state feedback. State estimates are obtained from a Kalman filter.

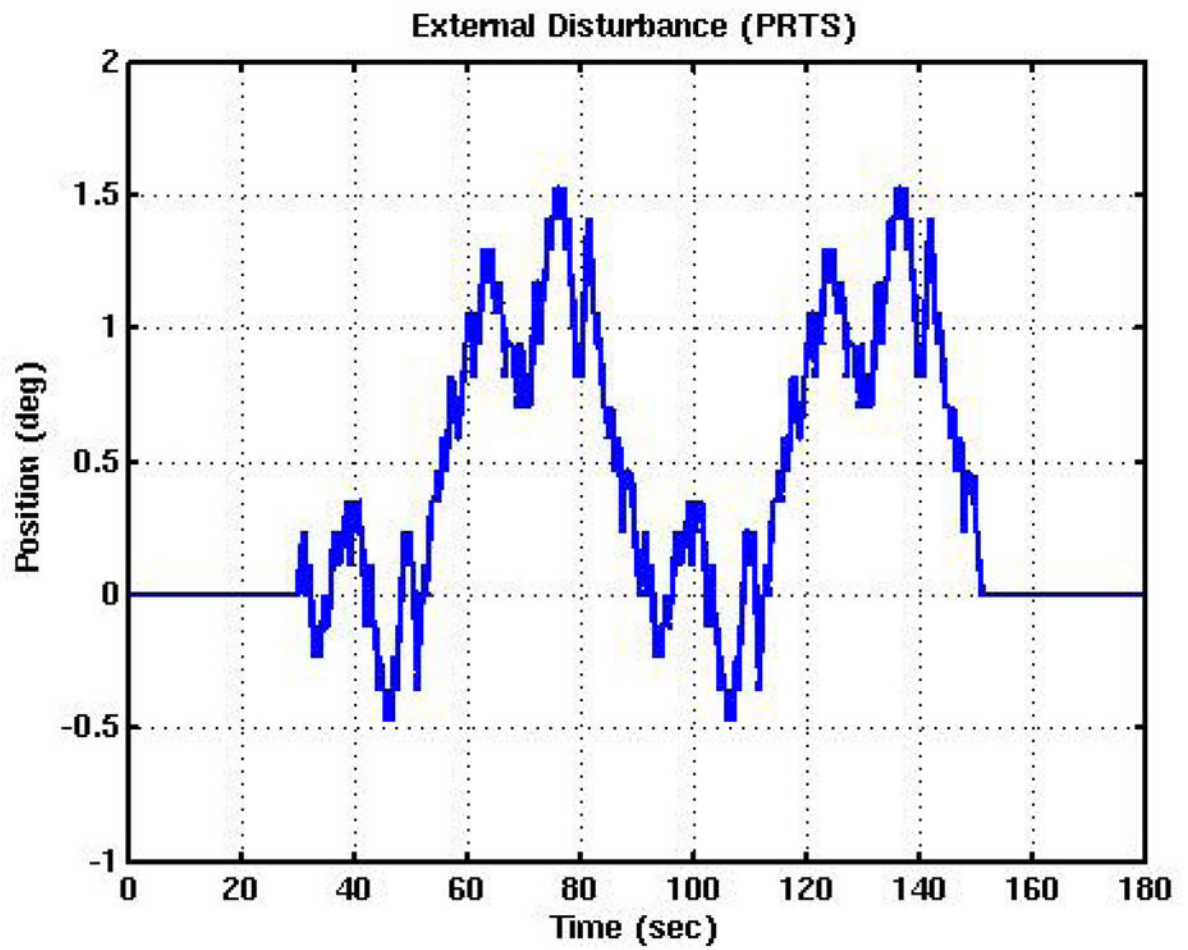


Fig. 6.
External disturbance applied to the ankle in the simulation.

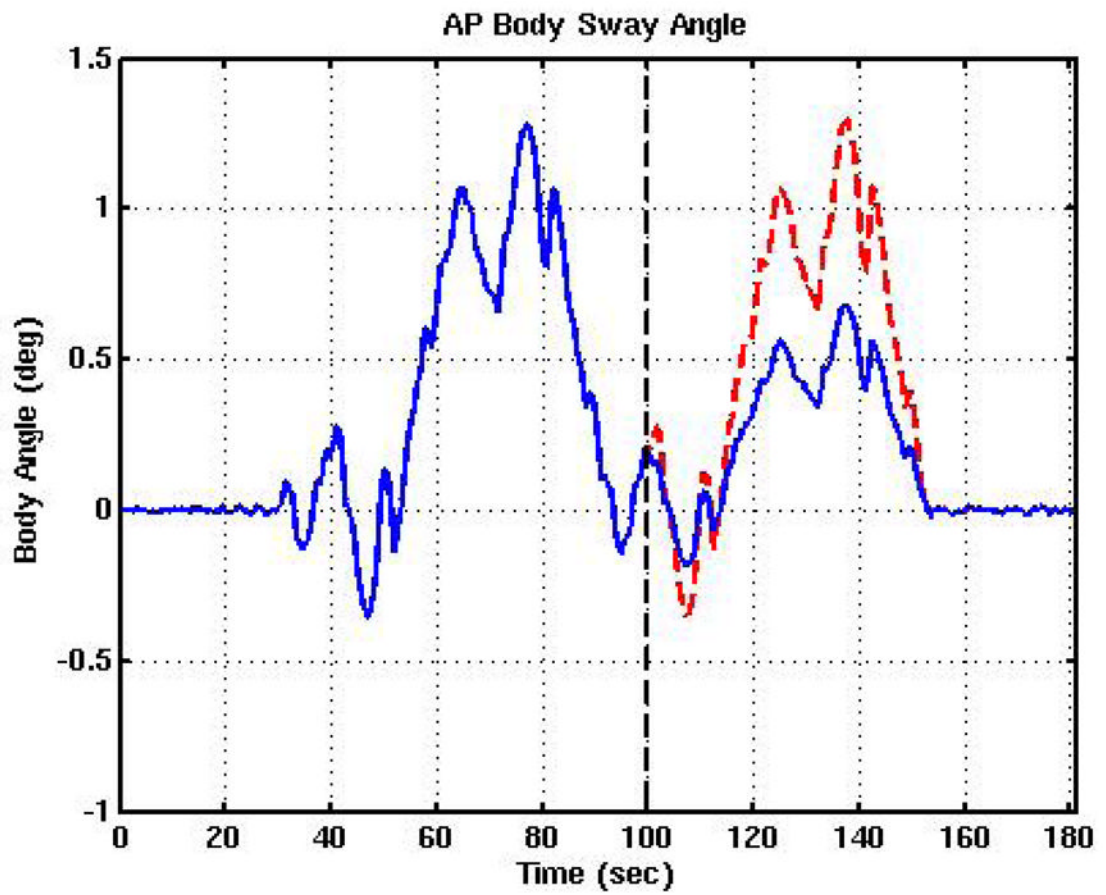


Fig. 7. Model response to a 2° peak-to-peak PRTS for no sensory re-weighting (dashed red trace) versus sensory re-weighting (solid blue trace). The vertical dashed line indicates onset of sensory re-weighting.

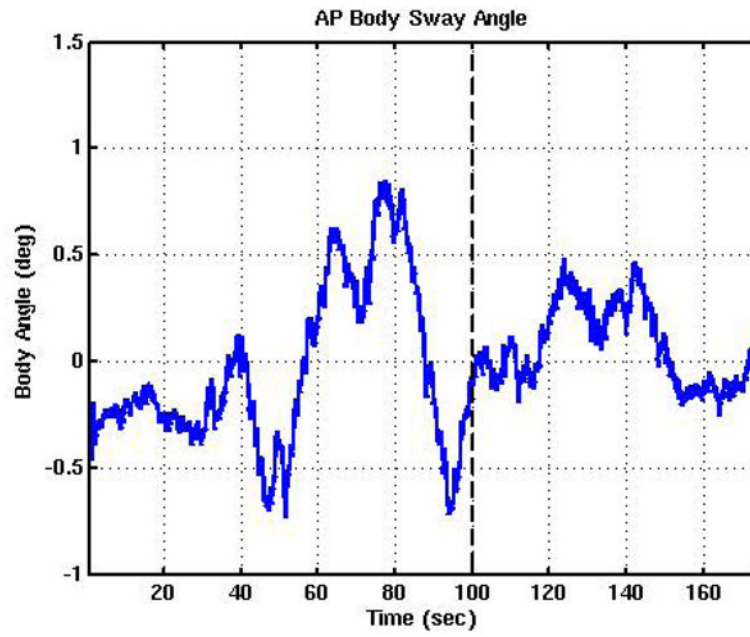


Fig. 8. Robot response to the same 2° peak-to-peak PRTS with sensory re-weighting. The vertical dashed line indicates onset of sensory re-weighting.